John von Neumann Institute for Computing

Modeling Si/B/N/(C) Ceramic Materials

Marcus Gastreich, Silke Reinhardt, Markus Doerr,
Christel M. Marian

published in

NIC Symposium 2001, Proceedings,
Horst Rollnik, Dietrich Wolf (Editor),
John von Neumann Institute for Computing, Jülich,
NIC Series, Vol. **9**, ISBN 3-00-009055-X, pp. 123-134, 2002.

http://www.fz-juelich.de/nic-series/volume9

Modeling Si/B/N/(C) Ceramic Materials

Marcus Gastreich[1], **Silke Reinhardt**[1], **Markus Doerr**[1], **and Christel M. Marian**[1,2]

[1] Fraunhofer Institut Algorithmen und Wissenschaftliches Rechnen (SCAI)
Schloss Birlinghoven, 53754 St. Augustin, Germany
E-mail: {marcus.gastreich, silke.reinhardt, markus.doerr, christel.marian}@scai.fhg.de

[2] Institut für Theoretische Chemie, Heinrich-Heine-Universität
Universitätsstr. 1, 40225 Düsseldorf, Germany
E-mail: marian@theochem.uni-duesseldorf.de

1 Introduction

Boron nitride and silicon nitride exhibit a diversity of industrial applications.[1–3] A combination of both, i.e., a material in the system Si/B/N promised to have a higher temperature resistance and to generally exhibit a lower tendency to crystallize. In fact, an *amorphous* solid with the desired properties was synthesized from molecular precursors in the 1990ies by Martin Jansen and coworkers.[4] Since that time, a variety of precursor derived Si/B/N/C ceramics have been developed.[5–10] Some of the carbon containing polyborosilazanes can even be spun and drawn to fibers. These ceramics are supposed to have great potential as working materials.[11–13]

For amorphous compounds as the above ones, structural data is extremely hard to extract solely from experiment. To aid the structural analysis, we have pursued three complementary approaches:

1. Quantum chemical investigation of the mechanisms and energetics of initial polymerization reactions
2. Computer simulation of the amorphous solid state and comparison of bulk properties
3. *Ab initio* calculation of local properties and set-up of quantitative structure-property relations (QSPR)

In the following, we shall give a brief survey over our contributions to the structural modeling of amorphous Si/B/N/(C) materials and of their genesis.

2 Reactions of Molecular Precursors

[(Trichlorosilyl)amino-dichloro]borane (TADB) and [(trichlorosilyl)dichloroboryl]ethane (TSDE) are two prominent molecular precursors for SiBNC ceramics (see Fig. 1). Both carry a silicon trichloride and a boron dichloride functional group. Typically, these molecular precursors are concatenated by liquid amines under cleavage of B-Cl or Si-Cl bonds (aminolysis) to yield larger molecular and polymeric units. Cross-linkage of the latter to form a three-dimensional SiBN(C) network is believed to occur at high temperatures, when the polymers are pyrolized ("burnt"). TADB and TSDE are multifunctional molecules.

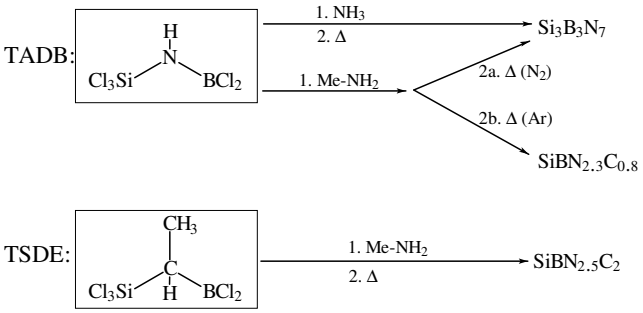

Figure 1. Synthesis of borosilazanes from molecular precursors via the polymer route (schematic).

Thus, besides N-attack at Si or B, many different reactions may occur leading to differently linked polymers and eventually to different microscopic distributions of elements in the solid.

What are the mechanisms and heat of reactions for an aminolysis of an Si-Cl and a B–Cl bond? Can the central nitrogen in the Si–N–B unit act as a Lewis base and cause a cross-link or branching of the molecular backbone? What is the probability of further aminolysis reactions with the solvent compared to a linkage of the monomeric units? Does the latter occur statistically via boron and silicon or is there a preference for one or the other side? Can the central Si–N–B and Si–C–B units break up upon aminolysis of the Si–Cl and B–Cl bonds? How do reaction conditions (solvent, temperature) influence the polymerization? In the following, we will try to give an answer to a few questions arising in this context.

2.1 BCl_3 and NH_3

To get a first idea of the reaction mechanism during the polymerization process, we began with the less complicated case of the ammonolysis of BCl_3 studied by means of quantum chemical methods.[14,15]

In the gas phase, i.e., for BCl_3 reacting with a single NH_3 molecule, the reaction coordinate is intuitively clear. Furthermore, entropic contributions are supposed to play a minor role. Therefore, time-independent methods can be employed to determine the course of the reaction. Minima and saddle points were located on the potential energy surface by roughly scanning along the constrained minimum energy path followed by BFGS searches.[14] Energies were computed at the level of second-order Møller-Plesset perturbation theory (MP2) using the Turbomole program package.[16] (Density functional theory (DFT) yields similar total reaction energies and barrier heights as MP2, but severely underestimates adduct formation energies.) In the course of the reaction, firstly a very stable adduct $H_3N{\cdot}BCl_3$ with four-fold coordinated N and B atoms is formed. The subsequent elimination of HCl is endothermic with respect to the adduct and proceeds via a high-lying transition state and a hydrogen-bonded complex. Overall, the first and second ammonolyses of BCl_3 are exothermic whereas the substitution of the last chlorine atom for an amino group is slightly endothermic in the gas phase (not shown).

When BCl_3 is dropped into liquid ammonia, more than one NH_3 molecule will participate in the reactions. Furthermore, ammonia is a polar solvent and thus preferentially stabilizes ionic or highly polar states. We have studied the mechanism and the energetic course of the substitution of a first chlorine atom of BCl_3 in the presence of eleven NH_3 molecules under periodic boundary conditions (PBC).[15] In this case, the reaction path and mechanism cannot be foreseen. To obtain an unbiased picture, we allowed the system to evolve in time without constraints by means of Car-Parrinello molecular dynamics (CPMD).[17] All CPMD simulations were performed using the massively parallelized Car-Parrinello program, version 3.0h,[18] as installed on the Cray T3E at the NIC. The solvent is found to have a strong

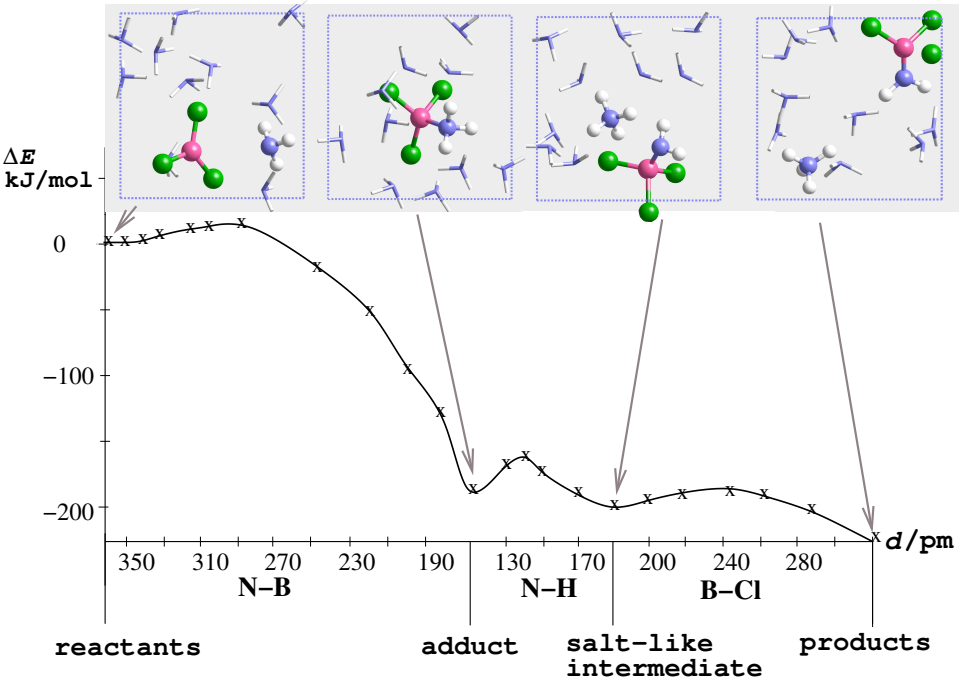

Figure 2. Minimum energy path of the ammonolysis of BCl_3 in the presence of eleven ammonia molecules and with PBC-treatment.

influence on both, the energetic course and the mechanism of the reaction (see Fig. 2). In the presence of ten additional ammonia molecules, the first ammonolysis releases 219 $kJ{\cdot}mol^{-1}$ compared to 50 $kJ{\cdot}mol^{-1}$ in the gas phase. Furthermore, every single step is exothermic: Formation of a boron trichloride ammonia adduct [$Cl_3B{\cdot}NH_3$], proton transfer yielding a salt-like intermediate [NH_4^+][$Cl_3BNH_2^-$], and elimination of a chloride ion leading to the products BCl_2NH_2 and [NH_4^+]Cl^-. All the intermediates and products are stabilized through hydrogen bonds with solvent ammonia molecules. Contrary to the gas phase reaction, the adduct formation proceeds via a transition state. The existence of such a (small) barrier is easily explained: The nitrogen lone-pair of the adduct-forming NH_3 molecule has to be resolved from the H-bonded network before it can attack the Lewis acid BCl_3. Once this barrier has been overcome, the reaction completes within picoseconds.

2.2 TADB and NH_3

As a next case, we studied reactions between the molecular precursor TADB and NH_3. Let us firstly concentrate on the gas phase results.[19] As expected, the main primary reaction is a substitution of a chlorine atom for an amino group at the boron center, the major product being (trichlorosilyl)(aminochloroboryl)amine (TACBA). If equal amounts of TADB and NH_3 are present, the further course of reaction is dominated by the oligomerization of TACBA to form very stable trimers with fourfold coordinated B and N. Elongation and branching of the Si–N–B backbone occur preferably after a single ammonolysis of a B–Cl or Si–Cl bond of the molecular precursor because the Lewis acidity of boron and silicon diminishes with an increasing number of amino substituents. Probable side reactions are processes during which the Si–N–B unit of the precursor opens up. Among the latter is the dissociation of the $H_3N{\cdot}BCl_2NHSiCl_3$ adduct to yield BCl_2NH_2 and $SiCl_3NH_2$ and the attack of the central amino group of TACBA at the boron center of another TADB in which bis[(trichlorosilyl)amino]chloroborane (TACB) and BCl_3 are formed. Both reactions lead to a segregation of boron-rich and silicon-rich regions. It is for these reasons that TADB is not suited as a molecular precursor for the chemical vapor deposition of homogeneous borosilazane ceramic coatings.

The transition states of all the above mentioned substitution reactions are more polar than the reactants and will thus be stabilized if the polymerization is conducted in liquid ammonia.[20] HCl eliminations are particularly favored by additional ammonia molecules: not only are their reaction barriers lowered markedly, their heats of reaction increase significantly due to the formation of NH_4Cl. For this reason, they are considerably enhanced over dissociation reactions and oligomerizations. In solution, the substitution of a chlorine atom for an amino group at the boron side of TADB remains the major primary process. The side reaction (i.e., the $H_3N{\cdot}BCl_2NHSiCl_3$ dissociation into BCl_2NH_2 and $SiCl_3NH_2$) is suppressed by an excess of ammonia. An important process in the continuing stage is a second ammonolysis at the boron side of TACBA. Finally, there is an indication for a preferred linkage of the monomeric TACBAs via their boron sides. Apart from the sequence just depicted, borazine rings are found to be particularly stable and should therefore be a frequent motif in the covalent network. Si–N–Si links are assumed to be formed at a later stage when the polymer is pyrolized. The preferred elongation of the polymer backbone via boron and the formation of borazine derivates probably leads to a non-uniform microscopic distribution of boron and silicon in the final ceramic. Indeed, recent ^{11}B-$\{^{29}Si\}$-REDOR NMR experiments support these assumptions.[21]

2.3 TSDE and Methylamine

Very recently, we started to look at the initial reactions of the molecular precursors TSDE (see Fig. 1) and methylamine which lead to an SiBNC ceramic with very high temperature resistance (2100°C). We present here only preliminary results of these quantum chemical investigations.[22] The mechanisms of the aminolysis reactions between NH_2CH_3 and TSDE in the *gas phase* closely resemble those of the TADB ammonolysis. However, comparing the energetic courses, marked differences are observed: The formation of adducts and products during the TSDE aminolysis yields much more energy and the reaction barriers are considerably lower. These trends can be explained by the fact that TSDE contains a saturated ethyl central unit whereas the Lewis acidity of boron and silicon in TADB is

reduced due the partial double bond character of the Si–N–B unit. The transition state for the HCl elimination at the boron side of TSDE is located even below the reactants. A possible side reaction is again the destruction of the original monomer unit.

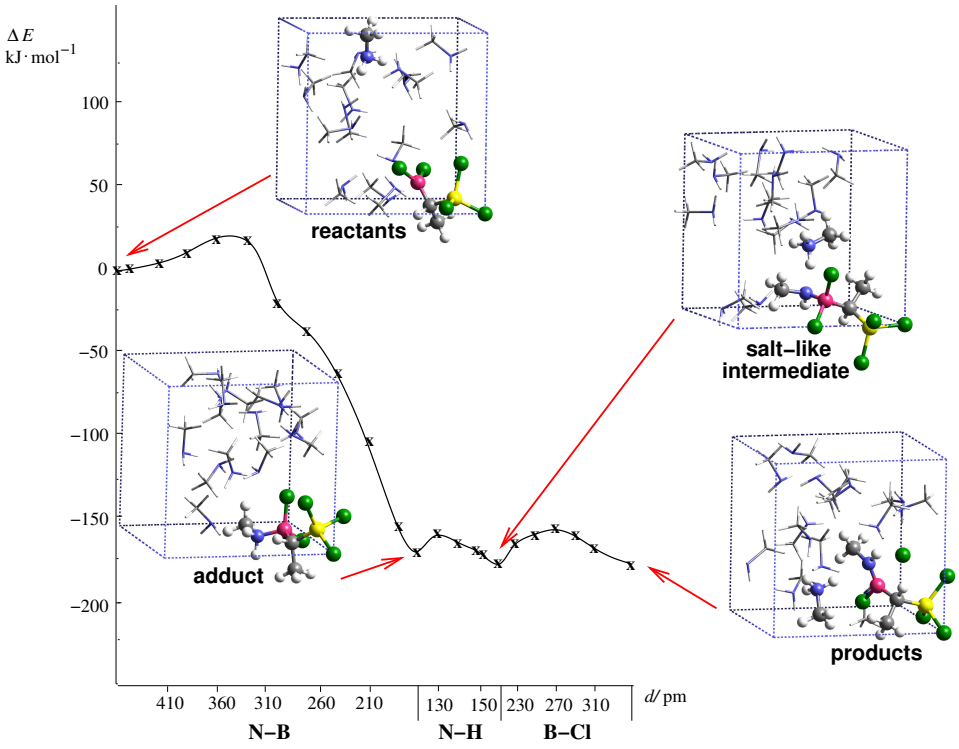

Figure 3. Simulation of the aminolysis of [(trichlorosilyl)dichloroboryl]ethane by liquid NH_2CH_3.

Solvent effects have been taken into account by treating the reaction of TSDE with 15 NH_2CH_3 in a periodic box. So far, however, limited simulation times have prevented the observation of a spontaneous reaction during the CPMD modeling. Instead, we have calculated a constrained minimum energy path for the aminolysis of TSDE, assuming a reaction mechanism similar to the one observed in the model system BCl_3 + 10 NH_3 (see Section 2.1). In an excess of NH_2CH_3, the overall reaction releases 176 kJ·mol^{-1} and is thus considerably more exothermic than in the gas phase (51 kJ·mol^{-1} without zero-point vibrational energy corrections). Furthermore, reaction barriers are of the order of 20 kJ·mol^{-1} and should easily be overcome. The contrary is true for the B–C-cleavage of the adduct into BCl_2NHCH_3 and $SiCl_3CH_2CH_3$. This reaction is much less exothermic than in the gas phase (22 kJ·mol^{-1} vs. 116 kJ·mol^{-1}). Also the transition state is destabilized as it requires the migration of a proton or hydrogen atom from the amino nitrogen to the ethyl carbon. It can therefore be safely assumed that this side reaction is suppressed in solution. Presently, we are investigating the most important entropic effects on the aminolysis reaction by thermodynamic integration along the constrained minimum energy path (blue moon ensemble[23]).

3 Parametrization and Validation of Classical Force Fields

Structural models for solids are either isolated clusters or periodically repeated units. In the case of amorphous materials, one has to compensate for the faulty assumption of periodicity by large unit cells. Otherwise, the amorphous character would not be grasped at all. On the other hand, for cluster models, longe-range order is not an issue, but small aggregates easily suffer from surface effects. Thus, unit cells and clusters favorably comprise thousands of atoms. Despite the progress of *ab initio* molecular dynamics methods in this field,[24] *ab initio* studies of $Si_3B_3N_7$ employing unit cells of this size are presently out of reach. Also, systematic global optimization procedures are not feasible which is why the phase space is sampled by classical molecular dynamics (MD) or Monte Carlo (MC) simulations. The latter require a predetermined expression for the potential energy, that is: a cost function. When the SFB 408 was founded, analytical interaction potentials for ternary Si/B/N compounds were not available in the literature. One of the initial stages of such computer modelling was thus the parameterization of an appropriate classical force field.

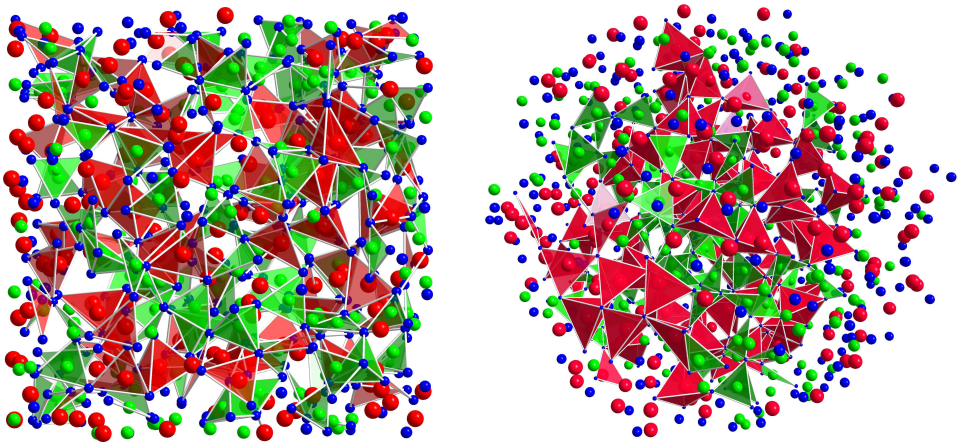

Figure 4. Periodic (left) and cluster (right) model of amorphous $Si_3B_3N_7$ (red: silicon, green: boron, blue: nitrogen). Coordination polyhedra are indicated for silicon and boron only.

Boron, nitrogen, and silicon are typical network building elements; bonding in solid boron nitride, silicon nitride, and borosilazane compounds exhibits partially ionic and partially covalent character. Ionic bonding is dominated by long-range Coulomb attraction and short-range Pauli repulsion. Both are isotropic in space, i.e., they do not depend on the position coordinates of two particles but only on their distance. Covalent bonding, on the other hand, involves directional forces. In a classical force field, these are typically represented by three-body interaction terms. The presence of three-body potentials in general improves force constants and other second-order properties of covalent compounds (vibrational properties, phonons, bulk moduli etc.). A complication arises when the coordination number varies for a pair of elements during simulations because three-body terms

are biased towards a certain bond angle and concomitantly towards a particular atomic coordination. It is thus extremely difficult to parameterize an interaction potential including three-body terms which simultaneously reproduces structures and second-order properties of differently coordinated modifications of a substance.

For solid state simulation, there occurs another principal difference to classical (harmonic) force fields: In the molecular modeling of organic and biochemical compounds, typically different parameter sets are utilized for different coordinations. This procedure implies that covalent bonds are neither broken nor built in the course of the simulation. The situation is different for ceramics: these materials are synthesized at high temperatures, and bond breaking and bond formation therefore have to be part of the modeling. Further, in amorphous networks such as borosilazanes, irregularities may occur; NMR spectra of amorphous $Si_3B_3N_7$ indicated that the prevailing boron and nitrogen coordination is trigonal and that silicon is mostly tetrahedrally surrounded in this material,[25] but under- and over-coordinations should not be ruled out in general.

Three different potentials have been parametrized for the modeling of Si/B/N/(H) compounds, labeled by $\mathcal{Q}$[26], $\mathcal{TB}$[27], and $\mathcal{WAT}+\mathcal{H}$[28]. The potential $\mathcal{Q}$ is based on a charged model for Si/B/N compounds. The assignment of effective charges is necessary for the determination of dipoles and associated properties, such as infra-red intensities and possible splittings between longitudinal and transversal optical phonon modes (LO/TO splittings). On the other hand, long-ranged Coulomb interactions require infinite summation techniques which add considerable complexity to a computer simulation and slow it down. $\mathcal{TB}$[27] and $\mathcal{WAT}+\mathcal{H}$[28] refrain from introducing explicit charges. Instead, Coulomb repulsions between Si–Si, B–B, N–N, and B–Si atomic pairs are mimicked by exponentially damped $1/r$-type potentials. By construction, these are short-ranged and avoid Ewald summation procedures. The potential energy functions acting between Si–N and B–N are expressed as Morse potentials. In order to obtain the proper layer structures of hexagonal and rhombohedral BN we included nitrogen-nitrogen dispersion interactions. The potential $\mathcal{WAT}+\mathcal{H}$ is particular in the sense that it additionally contains energy functions describing N–H, B–H, and Si–H bonds. For the parametrization of these energy functions, geometrical structures and harmonic vibrational frequencies of molecular amines, boranes, silanes, borazines, etc. were computed by means of density functional theory.

The parameters of the energy expressions are fitted to reproduce properties of molecules and crystals in a training set which ideally is sufficiently broad to yield transferable interaction potentials. All fitting has been performed using the GULP program.[29] We fit at constant-pressure and zero-temperature conditions using a weighted least squares procedure. Observables are either physical properties such as binding energies, vibrational frequencies etc. or structural data. Wherever applicable — i.e., in regions in which a structural relaxation results in a positive definite Hessian — the relax fitting mechanism has been employed; in this fitting mode crystalline or molecular structures are optimized at every step, and coordinates are taken as observables instead of forces.[30] Detailed information on molecular and solid state reference data and on our selection concerning the separation of the data set utilized for the training or the test of the force-field parameters may be found in the respective publications.[26–28]

To get an impression of the quality of the potentials, let us give some examples for validation studies. All potentials reproduce the structures with very low root mean square deviation (RMSD) values; for example, the $\mathcal{Q}$-model considering 279 observables leads

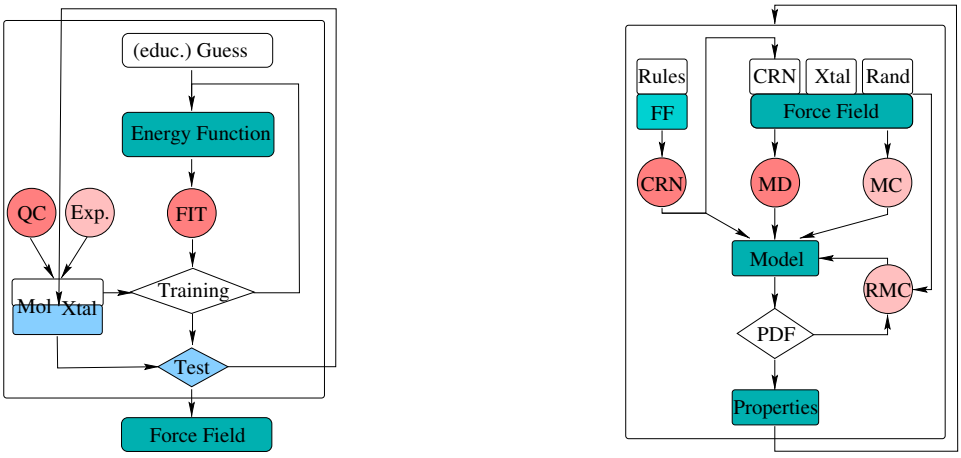

Figure 5. Parametrization and validation of a classical potential for the modeling of amorphous solids (left) and its application in continuous random network (CRN), molecular dynamics (MD), Monte Carlo (MC), and reverse Monte Carlo (RMC) procedures (right).

to an RMSD of 0.011879 Å. If one loosens the constraint of conserving symmetry of the (crystalline) test set, the value amounts to 0.01269 Å — whilst having to take into account 663 observables. The other potentials behave similarly, with limited loss of accuracy (not shown) due to the neglect of explicit charges. Besides structures, second-order properties usually are good targets for validation purposes. Such properties are important because they are related to the acceleration of particles in simulations. Thus, especially vibrational data and bulk moduli represent often-seen test cases. Being the potential with the highest evaluation time, the charged particle potential $\mathcal{Q}$ exhibits the most-transferable description of second-order properties.

An energy function is tested in a tougher way when applied to the description of *dynamic* properties. The standard validation scenario is the comparison of radial distribution functions from experiment with a theoretical one obtained after an MD simulation or other optimization techniques. We paradigmatically show this in Figure 6 for a 979-atomic cluster model of $Si_3B_3N_7$ giving reference to some of the available experimental sources in the SFB 408. It has to be taken into account that different elements scatter differently and as a function of the radiation used; this is why the intensity for some of the peaks differs between the transmission electron microscopy (TEM) results and the ones from X-ray experiments. In our case, we treated the theoretical data to be comparable to X-ray experiments. It can be seen that the distance region to around 3.5 Å is well reproduced by all potentials. The early signals are sharp and at distances where one expects them (typical B–N bond around 1.44 Å, typical Si–N bond around 1.72 Å). There are no artifacts demonstrating the robustness of the potentials employed. Higher distances are less accurately calculated which is mainly due to the fact that the model is relatively small (radius $\approx$ 10 Å) — here, we do not aim at establishing a definite structural model for $Si_3B_3N_7$. It is beyond the scope of this article to also document the overlapping signals in inverse space which is often done to document the validity of the cost function in terms of long-

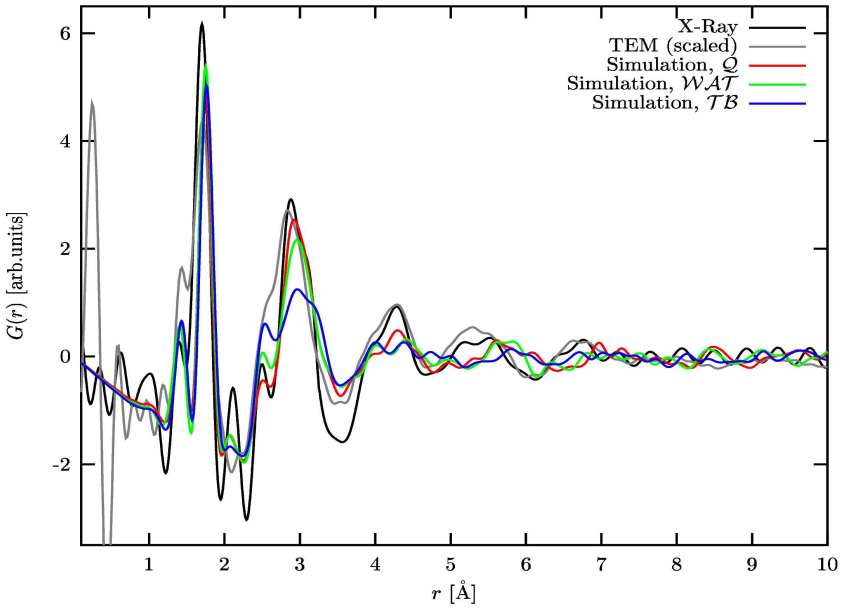

Figure 6. Radial distribution functions of $Si_3B_3N_7$ cluster models optimized with the potentials $\mathcal{Q}$, $\mathcal{TB}$, or $\mathcal{WAT}$ in comparison with experiments on the ceramic material. The signal at 2.1 Å in the X-ray experiment is mainly due to the Fourier transformation of the inverse-space data as are the wiggles below 1.2 Å.

range forces. All in all, today, we have three (four if hydrogen is taken into account) cost functions at hand; the application purposes determine the amount of tradeoff which has to be made on the side of either time or accuracy.

4 Parametrization of NMR Chemical Shifts and Reverse Monte Carlo Refinement

Another valuable for the exploration of the structure of amorphous solids are NMR experiments. We could demonstrate that especially the N chemical shift is very sensitive to changes in the local environment around this atom.[31] NMR chemical shifts can nowadays be calculated with sufficient accuracy at the *ab initio* level of theory. These calculations are limited however to systems with less than about 100 atoms. Even compounds of that size required the facilities at NIC. In addition, such methods are not directly applicable to structural models for amorphous solids (which usually contain several thousands of atoms). To be of use, we have parametrized the chemical shift δ as a function of the local structure. We trained the fit with *ab initio* calculations on smaller clusters containing 40-70 atoms. We started out with the binary system BN; all clusters were hydrogen-saturated cut-outs of the crystals hex- and cubic BN. Clusters were enlarged to convergence of δ for central N atoms so that we were able to predict the formerly unknown $\delta(^{15}N)$ for hexagonal boron nitride. The calculated chemical shifts agree within a few ppm with an experiment that was conducted half a year later by Jeschke *et al* in the framework of the SFB 408.[32] Calculations on Si_3N_4, the other binary subsystem of $Si_3B_3N_7$, show that the N chemical shift in

this system should be parametrizable in a similar way.

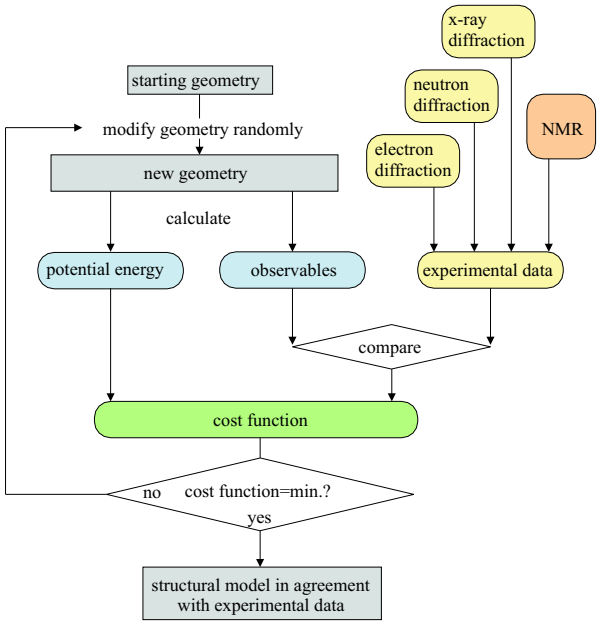

Figure 7. Generation of a structural model in a Reverse Monte Carlo procedure.

A widely used approach for the refinement of structural models for amorphous solids is the Reverse Monte Carlo method. Basic idea of this method is to modify a structural model randomly until the properties calculated from this model agree as good as possible with experimental data. Experimental data is usually taken from diffraction experiments (X-ray, neutron, or electron). As such data represent 1D-projections of a 3D structure, there emerge ambiguities w.r.t. the generated structure model. To overcome this shortcoming, it is desirable to take as much information into account as possible. A standard procedure is to limit the solution space to energetically accessible structures — evaluated by the $\mathcal{TB}$-potential in our case. An obvious improvement then is to further augment the cost function by NMR information. As a first test case, we are currently applying this scheme to amorphous BN.

Acknowledgments

We would like to dedicate this article to the memory of Attila Çağlar, a colleague from the SFB 408, who died much too early at the age of 33. We have very much appreciated him as one of the first researchers to employ our potentials in his work on BN-nanotubes and are grateful having experienced his open mindedness. He will be deeply missed.

This work has been funded by the Deutsche Forschungsgemeinschaft in the framework of Sonderforschungsbereich 408 “Anorganische Festkörper ohne Translationssymmerie”.

We thank the John von Neumann Institute for Computing in Jülich for the allocation of computing time and technical support — especially Drs. Johannes Grotendorst and Norbert Attig.

References

1. F. Aldinger. *Werkstoffe, die die Welt verändern – Hochleistungskeramiken machen den etablierten Materialien Konkurrenz*, Physikalische Blätter **55**, 31–37 (1999).
2. A. V. Blinder, A. S. Bolgar, and V. Y. Petrovskii. *Thermophysical properties of materials based on silicon nitride*, Powder Metall. Met. Ceram. **34**, 151–154 (1995).
3. N. Hirosaki, Y. Okamoto, M. Ando, F. Munakata, and Y. Akimune. *Thermal Conductivity of gas-pressure-sintered Silicon Nitride*, J. Amer. Ceram. Soc. **79**, 2878–2882 (1996).
4. H.-P. Baldus, O. Wagner, and M. Jansen. *Synthesis of Advanced Ceramics in the Systems Si–B–N and Si–B–N–C Employing Novel Precursor Compounds*, Mat. Res. Soc. Symp. Proc. **271**, 821–826 (1992).
5. Hardy Jüngermann. *Molekulare und polymere Vorläufer für quaternäre Keramiken im System Si/B/N/C*. Doctoral thesis, Bonn University (1997).
6. Utz Müller. *Amorphe Keramiken im System Si/B/N/(C) Synthese neuer Einkomponentenvorläufer und Keramiken; Aufklärung neuer Strukturcharakteristika durch isotope Substitution*. Doctoral thesis, Bonn University (2000).
7. Matthias Kroschel. *Amorphe B/Si/C/N-Hochleistungskeramiken aus Einkomponentenvorläufern*. Doctoral thesis, Bonn University (2001).
8. D. Srivastava, E. N. Duesler, and R. T. Paine. *Synthesis of Silylborazines and Their Utilization as Precursors to Silicon-Containing Boron Nitride*, Eur. J. Inorg. Chem., 855–859 (1998).
9. E. Kroke and Y.-L. Li and C. Konetschny and E. Lecomte and C. Fasel and R. Riedel. *Silazane derived ceramics and related materials*, Mat. Sci. Eng. R: Reports, **26** 97–199 (2000).
10. Joachim Bill and Fumihiro Wakai and Fritz Aldinger, eds. *Precursor-Derived Ceramics*, Wiley-VCH (1999).
11. H.-P. Baldus and M. Jansen. *Temperaturbeständige Keramikfasern – Eine heiße Geschichte*, Bayer Research **10**, 46 (1998).
12. H.-P. Baldus and M. Jansen. *High-Performance Ceramics — Amorphous Inorganic Networks from Molecular Precursors*, Angew. Chem. Int. Ed. Engl. **36**, 328–343 (1997).
13. H.-P. Baldus, M. Jansen, and D. Sporn. *Ceramic Fibers for Matrix Composites in High-Temperature Engine Applications*, Science **285**, 699–703 (1999).
14. S. Reinhardt, M. Gastreich, and C. M. Marian. *Reactions in the initial stage of the CVD of BN — a quantum chemical investigation*, Phys. Chem. Chem. Phys. **2**, 955 (2000).
15. S. Reinhardt, C.M. Marian, and I. Frank. *The influence of excess ammonia on the mechanism of the reaction of boron trichloride with ammonia — An ab initio molecular dynamics study*, Angew. Chem. **113(19)**, 3795 (2001).
16. Karlsruhe Quantum Chemistry Group.
`http://www.chemie.uni-karlsruhe.de/PC/TheoChem`
Turbomole homepage.

17. R. Car and M. Parrinello. *Unified approach for molecular dynamics and density-functional theory*, Phys. Rev. Lett. **55**, 2471 (1985).
18. J. Hutter et al. *CPMD*. Max-Planck-Institut für Festkörperforschung and IBM Research (1990 – 1996).
19. S. Reinhardt, M. Gastreich, and C.M. Marian. *Quantum chemical investigation of initial reactions between the molecular precusors TADB and ammonia I: Gas phase reactions*, J. Phys. Chem. A (2001), accepted.
20. S. Reinhardt, M. Gastreich, and C.M. Marian. *Quantum chemical investigation of initial reactions between the molecular precusors TADB and ammonia II: Solvent effects*, in preparation (2001).
21. L. van Wüllen, U. Müller, and M. Jansen. *Understanding Intermediate-Range Order in Amorphous Nitridic Ceramics: A $^{29}Si\{^{11}B\}$ REDOR/READPOR and $^{11}B\{^{29}Si\}$ REDOR Study*, Chem. Mater. **12**, 2347 (2000).
22. M. Gastreich, C.M. Marian, H. Jüngermann, and M. Jansen. *Molecular Precursors to Ceramics II: [(Trichlorosilyl)dichloroboryl]ethane: Synthesis and Characterization by Means of Experiment and Theory*, Eur. J. Inorg. Chem. **(1)**, 75–81 (1999).
23. M. Sprik and G. Ciccotti. *Free energy from constrained molecular dynamics*, J. Chem. Phys **109(180)**, 7737-7744 (1998).
24. A. Çağlar and M. Griebel. *On the Numerical Simulation of Fullerene Nanotubes: $C_{100.000.000}$ and Beyond!* in: Workshop on Molecular Dynamics on Parallel Computers, Rüdiger Esser, Peter Grassberger, Johannes Grotendorst, and Marius Lewerenz (Ed.), World Scientific, Singapore, pages 5–31 (2000).
25. U. Müller, W. Hoffbauer, and M. Jansen. *Short-Range Ordering in Amorphous $Si_3B_3N_7$ as Determined by Multinuclear NMR-Sectroscopy*, Chem. Mater. **12**, 2341–2346 (2000).
26. Marcus Gastreich. *Werkzeuge zur Modellierung von Siliciumbornitrid-Keramiken: Entwicklung von Mehrkörperpotenzialen und Berechnungen zur NMR-chemischen Verschiebung*. Doctoral thesis, Bonn University (2001).
27. C.M. Marian, M. Gastreich, and J.D. Gale. *Empirical two-body potential for solid silicon nitride, boron nitride, and borosilazane modifications*, Phys. Rev. B **62(5)**, 3117–3124 (2000).
28. C.M. Marian and M. Gastreich. *A systematic theoretical study of molecular Si/N, B/N, and Si/N/B compounds and parameterisation of a force-field for molecules and solids*, J. Mol. Struc.: Theochem **506**, 107–129 (2000).
29. J.D. Gale. *GULP: a computer program for the symmetry adapted simulation of solids*, J. Chem. Soc. Faraday Trans. **93**, 629, 1997.
30. J.D. Gale. *Empirical potential derivation for ionic materials*, Phil. Mag. B. **73**, 3 (1996).
31. M. Gastreich and C.M. Marian. *Quantitative Structure-Property Relationships in Boron Nitrides: The ^{15}N and ^{11}B Chemical Shifts*, Sol. State NMR **19** (1/2), 29–44 (2001).
32. G. Jeschke, W. Hoffbauer, and M. Jansen. *A comprehensive NMR study of cubic and hexagonal boron nitride*, J. Solid State NMR **12**, 1–7 (1998).